

A next-to-next-to-leading-order $pp \rightarrow pp^0$ Transition Operator in Chiral Perturbation Theory

V. Dmitrasinovic^a, K. Kubodera^a, F. Myhrer^a and T. Sato^b

^a Department of Physics and Astronomy, University of South Carolina
Columbia, SC 29208, U.S.A.

^b Department of Physics, Osaka University, Toyonaka, Osaka 560-0043, Japan
(February 5, 2020)

Abstract

We present a systematic analysis of next-to-next-to-leading-order diagrams that contribute to the $pp \rightarrow pp^0$ production at threshold. Analytic expressions are given for the effective transition operators, and the relative importance of various types of diagrams is discussed. The vertex-correction-type graphs are found to give only small corrections to lower order graphs in conformity with expectations. By contrast, we find very large contributions from the two-pion exchange graphs which can be interpreted as a part of effective meson exchange diagrams.

a. Introduction High-precision measurements [1,2] of neutral pion production in proton-proton collisions $pp \rightarrow pp^0$ just above the threshold have generated renewed theoretical scrutiny of this reaction [3]–[16]. This reaction is unique among two-nucleon pion production processes in that it is not well described by the single-nucleon process (Born term), Fig.1 (a), and the s-wave pion rescattering process, Fig.1 (b). The reason is that the "large" Weinberg-Tomozawa term does not contribute to the $pp \rightarrow pp^0$ reaction, in contrast with e.g. charged-pion production $pp \rightarrow pn^+$, thus rendering $pp \rightarrow pp^0$ particularly sensitive to and hence a perfect testing ground for the less-well-understood "small" isoscalar s-wave pion rescattering terms. From the calculations done thus far it is clear that the two most basic processes, Fig.1 (a) and 1 (b), give much smaller $pp \rightarrow pp^0$ cross sections than the measured ones. Lee and Riska's model calculation [4] suggests that shorter range isoscalar meson-exchange processes, like the π - and η -exchanges between the two protons, might be very important for this reaction.

In heavy-baryon chiral perturbation theory [HB χ PT] [17] one can define the "large" and "small" terms in the Hamiltonian by way of chiral-order counting.¹ In this language the first pion rescattering contributions to $pp \rightarrow pp^0$ are one chiral-order higher than those of the charged-pion production (e.g., $pp \rightarrow pn^+$). This means that $pp \rightarrow pp^0$ production

¹ Extension of HB χ PT to cases with two or more nucleons is not unique, however: Cohen et al. [14] have proposed a modification of Weinberg's chiral counting rules. We do not address this issue here but simply use the standard counting rules à la Weinberg [18].

is very sensitive to "correction terms", which tend to be "masked" by the leading terms in most low-energy pion-nucleon processes. Since the Born term and the pion rescattering term do not explain the cross section, we extend our previous calculation [13] to the next chiral order. The purpose of this note is two-fold: (a) to report analytic results for the transition operators that arise from a systematic treatment of the next chiral order diagrams; and (b) to compare their importance, at threshold, relative to the one-pion exchange rescattering graph, Fig.1(b).

In the present work we concentrate on calculations of the effective transition operator, without considering the initial- and final-state interactions in the transition amplitude. We are aware of the paramount importance of a full distorted-wave (DW) calculation for obtaining realistic transition amplitudes that can be directly compared with the experiment, but relegate this task to a forthcoming publication [19]. One reason for doing so is that the transition operators resulting from our systematic treatment of the new diagrams exhibit very complicated energy- and momentum-dependencies, rendering a full DW calculation a highly non-trivial numerical task. Secondly, it seems that an analysis of the transition operators themselves can shed light on the roles of higher chiral-order terms. Our most salient finding is that the two-pion exchange diagrams, which have no lower-order counterparts, give by far the most dominant transition operators (sometimes by an order of magnitude larger than the nominally "leading" ones). These diagrams being interpretable as part of an effective π -meson exchange (see below), our results, albeit subject to modification due to DW effects, give the first hint of a connection between ChPT and the phenomenological one-boson exchange models.

b. Conventions and other preliminaries The effective Lagrangian L_{ch} in HB χ PT is expanded as

$$L_{\text{ch}} = L^{(0)} + L^{(1)} + L^{(2)} + \dots \quad (1)$$

$L^{(n)}$ represents a term of chiral order $d + (n-2)$, where n is the number of fermion fields in the term, and d is the number of derivatives or powers of m_π . The explicit forms for the $n = 0$ and 1 terms are [20]:

$$L^{(0)} = \frac{f^2}{4} \text{Tr}[\partial_\mu U^\dagger \partial^\mu U + m_\pi^2 (U^\dagger + U - 2)] + N (iv \cdot D + g_S u) N \quad (2)$$

$$L^{(1)} = \frac{ig_A}{2m_N} N f S \cdot D ; v \cdot u g_N + \frac{1}{2} m_\pi^2 N N \text{Tr}(U + U^\dagger - 2) \\ + (c_2 \frac{g_A^2}{8m_N}) N (v \cdot u^2) N + c_3 N u \cdot u N + \dots \quad (3)$$

where we have retained only terms of direct relevance to our present calculation. The $SU(2)$ field matrix $U(x)$ is non-linearly related to the pion field and has standard chiral transformation properties. We use the representation $U(x) = 1 + \frac{i}{f} \pi(x) + \frac{1}{f^2} \pi^2(x) + \dots$ as in Ref. [20]. $N(x)$ represents the large component of the heavy-nucleon field; the four-velocity parameter v is chosen to be $v = (1; 0; 0; 0)$; $D \cdot N = \partial_\mu N \cdot \frac{1}{2} v^\mu$; $\partial_\mu N$ is the covariant derivative of N ; S is the (covariant) spin operator, which in the nucleon rest frame becomes $S = (0; \vec{\sigma}/2)$, and $u = i[\partial_\mu U^\dagger \partial^\mu U - \frac{1}{2} (\partial_\mu U^\dagger)^2 - \frac{1}{2} (\partial_\mu U)^2]$, where $\partial_\mu U = \partial_\mu U(x)$ [20]. The low-energy constants c_1, c_2 and c_3 have been determined from other processes, see e.g. Refs. [15,20]. An

explicit expression for $L^{(2)}$, which includes $O(m_N^2)$ recoil terms as well as terms containing new low-energy constants, can be found, e.g., in Ref. [21].

In Weinberg's chiral counting [18] each irreducible Feynman diagram carries a chiral order index defined by $\chi = 4 - E_N - 2C + 2L + \sum_i i_i$, where E_N is the number of nucleons in the Feynman diagram, L the number of loops, C the number of disconnected parts of the diagram, and the sum runs over all the vertices in the Feynman graph [18]. In this note we consider irreducible diagrams with chiral orders up to $\chi = 2$ that give rise to $pp \rightarrow pp^0$ transition operators. These diagrams are shown in Figs. 1-5. In the following $T^{(\chi)}$ stands for a transition operator of chiral order χ . The lowest-order transition operator for the Born diagram [Fig.(1a)] has $\chi = 1$, and that for the rescattering diagram has $\chi = +1$ [Fig.(1b)]. We define the first HB χ PT calculation [13,14] which includes the aforementioned terms as the next-to-leading (NLO) calculation. Hence we decree our next chiral order ($\chi = 2$) calculation to be next-to-next-to-leading (NNLO) order. With the use of L_{ch} in Eq.(1), the two transition operators that feature in the NLO calculation are given (in momentum space) by [13,14]

$$T^{Born} = T^{(\chi=1)} = \frac{g_A}{2f} \sum_{j=1,2} \frac{!_q}{2m_N} \sim_j (\mathbf{p} + \mathbf{p}_j^0) \cdot \mathbf{k}_j; \quad (4)$$

$$T^{Resc} = T^{(\chi=+1)} = \frac{g_A}{f} \sum_{j=1,2} \frac{!_q}{k_j^2} \frac{\sim_j \cdot \mathbf{k}_j}{m^2 + i}; \quad (5)$$

where \mathbf{p}_j and \mathbf{p}_j^0 ($j = 1, 2$) denote the initial and final momenta of the j -th proton. The four-momentum of the exchanged pion is defined by the nucleon four-momenta at the NN vertex: $k_j = p_j - p_j^0$, where $p_j = (E_{p_j}; \mathbf{p}_j)$; $p_j^0 = (E_{p_j^0}; \mathbf{p}_j^0)$ with the definition $E_p = (\mathbf{p}^2 + m_N^2)^{1/2}$. The s -wave rescattering vertex function $\gamma(k; q)$ is calculated from Eq.(3):

$$\gamma(k; q) = \frac{m^2}{f^2} [2c_1 + (c_2 - \frac{g_A^2}{8m_N}) \frac{!_q k_0}{m^2} + c_3 \frac{q \cdot k}{m^2}]; \quad (6)$$

where $k = (k_0; \mathbf{k})$ and $q = (!_q; \mathbf{q})$ represent the four-momenta of the exchanged and final pions, respectively, and $!_q = (q^2 + m^2)^{1/2}$.

c. Analytic results When we consider NNLO, we find 19 topologically distinct new types of diagrams that can potentially contribute to $NN \rightarrow NN$ reactions. For a particular case of the $pp \rightarrow pp^0$ reaction near threshold, the isospin selection rules and the s -wave character of the outgoing pion reduce this number from 19 to 6. We refer to these six as Type I, Type II, ..., Type VI, and illustrate them in Figs. 2-4. Types I, II and III appear in Fig. 2, Type IV in Fig. 3, and Types V and VI in Fig. 4. Some of these diagrams have been considered by Gedalin et al. [22], as we shall discuss later. We denote by M_I, M_{II}, \dots , the NNLO transition operators that arise from the diagrams of Type I, II, ..., respectively. In addition to these six operators, as will be explained in more detail below, there is an NNLO contribution from Fig. 5, which looks the same as Fig. 1(b), but which constitutes a higher-order correction to $T^{(+1)}$ [eq.(5)]. We denote by M_{VII} the transition operator due to this correction. Then the total NNLO transition operator we consider is given by

$$T^{(+2)} = M_I + M_{II} + M_{III} + M_{IV} + M_V + M_{VI} + M_{VII}; \quad (7)$$

The explicit expressions for these operators are as follows. (In the expressions below the subscripts i and j refer to nucleon number 1 and 2.)

$$M_I = \frac{g_A}{8f^5} \sum_{i \neq j=1,2}^X S_i \cdot k [X_1 + \frac{X_2}{k_j^2}] \quad (8)$$

where

$$X_1 = v \cdot (p + p_i^0) I(k_j) + v \cdot (q + \frac{p_i^0}{2}) v \cdot (q + p + p_i^0) I_0(v \cdot p \cdot v \cdot k; k_j^2) + \\ + v \cdot (q \frac{p_i}{2}) v \cdot (q \cdot p \cdot p_i^0) I_0(v \cdot p \cdot v \cdot k; k_j^2) \quad (9)$$

$$X_2 = v \cdot (p + p_i^0) v \cdot (5q \cdot k \cdot v \cdot k I(k_j) - v \cdot (q + \frac{p_i^0}{2}) v \cdot (q + p + p_i^0) \\ [J_0(v \cdot p \cdot J_0(v \cdot (p + k_j)) + v \cdot k \cdot (k + 2p_i) I_0(v \cdot p \cdot v \cdot k; k_j^2)] + \\ v \cdot (q \frac{p_i}{2}) v \cdot (q \cdot p \cdot p_i^0) [J_0(v \cdot p \cdot J_0(v \cdot (p \cdot k_j)) + v \cdot k \cdot (k + 2p_i^0) I_0(v \cdot p \cdot v \cdot k; k_j^2)] : \quad (10)$$

$$M_{II} = \frac{g_A^3}{8f^5} \sum_{i \neq j=1,2}^X S_i \cdot (k \cdot k_i) f J_0(v \cdot p) + J_0(v \cdot p) + v \cdot (p + p_j^0) I(k_j) + \\ + (2m^2 + 2v \cdot p \cdot v \cdot p + k_j^2) I_0(v \cdot p \cdot v \cdot k; k_j^2) g : \quad (11)$$

$$M_{III} = \frac{g_A^3}{4f^5} \sum_{i \neq j=1,2}^X [S_i \cdot k X_1 + 2i \cdot v \cdot S_j \cdot S_i \cdot k_j X_2] : \quad (12)$$

where

$$X_1 = v \cdot (p + p_j + p_i^0 + p_j^0) \frac{1}{2} I(k_j) + \\ + \frac{1}{v \cdot (p \cdot p_j^0)} [v \cdot (p + q + k_j) Y(v \cdot p \cdot k_j) - v \cdot (p + q + k_j) Y(v \cdot p \cdot k_j)] + \\ + \frac{1}{v \cdot (p \cdot p_j)} [v \cdot (p \cdot q \cdot k_j) Y(v \cdot p \cdot k_j) - v \cdot (p \cdot q \cdot k_j) Y(v \cdot p \cdot k_j)] \quad (13)$$

$$X_2 = \frac{1}{v \cdot (p \cdot p_j^0)} [v \cdot (p + q + k_j) A(v \cdot p \cdot k_j) - v \cdot (p + q + k_j) A(v \cdot p \cdot k_j)] + \\ + \frac{1}{v \cdot (p \cdot p_j)} [v \cdot (p \cdot q \cdot k_j) A(v \cdot p \cdot k_j) - v \cdot (p \cdot q \cdot k_j) A(v \cdot p \cdot k_j)] : \quad (14)$$

In Eqs.(13) and (14):

$$Y(!; P) = \\ \frac{1}{4} [4(v \cdot P) I(P) - J_0(!) - J_0(! \cdot v \cdot P) + (2m^2 - 2(! \cdot v \cdot P)^2 + P^2) I_0(!; v \cdot P; P^2)] + \\ + \frac{[2m^2 - !^2 - (! \cdot v \cdot P)^2]}{4P^2} \\ [2(v \cdot P) I(P) - J_0(!) + J_0(! \cdot v \cdot P) + (v \cdot P) (2! \cdot v \cdot P_0 (!; v \cdot P; P^2))] : \quad (15)$$

and

$$\begin{aligned}
A(!;P) = & \frac{(2! - v P)P^2}{4P^2} I(P) + \\
& + \frac{m^2}{2} + \frac{P^2 P^2 + 4!^2 - 4! (v P)}{8P^2} I_0(!;v P;P^2) + \\
& + \frac{1}{4} J_0(! - v P) + \frac{P^2 - 2! (v P)}{8P^2} (J_0(!) - J_0(! - v P)) + \\
& + \frac{v P - 2!}{2(4)^2} + O(4-d):
\end{aligned} \tag{16}$$

$$\begin{aligned}
M_{IV} = & \frac{g_A^3}{4f^5} \sum_{i,j=1,2}^X \frac{S_j k_j}{k_j^2 m^2 + i} \\
& f m^2 + (v p^2 - J_0(v p + m^2 + (v p^2 - J_0(v p + \\
& + v (p + p_i^0) + 3k_i^2 m^2 - 2k_i q)X g;
\end{aligned} \tag{17}$$

where

$$\begin{aligned}
X = & \frac{v (p + p_i^0)}{2} I(k_i) + \\
& + m^2 - v p v p^0 - \frac{1}{2} k_i^2 - I_0(v p v k_i^2) - \frac{1}{2} [J_0(v p + J_0(v p^0)]:
\end{aligned} \tag{18}$$

$$\begin{aligned}
M_V = & \frac{g_A^3}{4f^5} \sum_{i,j=1,2}^X \frac{S_j k_j}{k_j^2 m^2 + i} \\
& f v (p + p_i^0) + ((v p^2 - m^2) J_0(v p + (v p^2 - m^2) J_0(v p^0) g;
\end{aligned} \tag{19}$$

$$\begin{aligned}
M_{VI} = & \frac{g_A}{8f^5} \sum_{i,j=1,2}^X \frac{S_j k_j}{k_j^2 m^2 + i} \\
& f v (p + p_i^0) + v (2q + p^0 v (k + 2q + p_i^0) J_0(v (p + q)) + \\
& + v (2q - p^0 v (k + 2q - p_i^0) J_0(v (p - q)) g;
\end{aligned} \tag{20}$$

As mentioned earlier, the graph in Fig 5 with the relevant lowest order vertices gives $T^{(+1)}$ [eq.(5)]. If we, however, use for the pion rescattering vertex in Fig 5 the lagrangian $L^{(2)}$ [21], there results an NNLO transition operator, M_{VII} , which represents "recoil" term corrections of $O(m_N^{-2})$ to $T^{(+1)}$. Its explicit expression is

$$M_{VII} = \frac{g_A}{f} \sum_{i,j=1,2}^X \frac{0_i(k_j; q) \frac{\sim_j k_j^0}{k_j^2 m^2 + i}}{k_j^2 m^2 + i} \tag{21}$$

where the expression for $0_i(k_j; q)$ is obtainable from Eq.(C 3) of Ref. [21].

The above expressions for the $= 2$ diagrams contain four independent one-loop integrals, $J_0(!)$, $I(P^2)$ and $I_0(!;v P;P^2)$, of which the first three contain divergences. The finite

parts are defined to include $\ln(m_N = 0)$. We choose the cut-off parameter to be $\Lambda = 1 \text{ GeV}$. The two integrals, $I_0(!)$ and $J_0(!)$, can be found in Ref. [20], while $I(P^2)$ is a standard Feynman integral:

$$I(P^2) = \frac{1}{i} \int \frac{d^4 l}{(2\pi)^4} \frac{1}{[m^2 - l^2 - i''] [m^2 - (l - P)^2 - i'']} : \quad (22)$$

The last integral, which is new, is given by

$$\begin{aligned} I_0(!; v \cdot P; P^2) &= \frac{1}{i} \int \frac{d^4 l}{(2\pi)^4} \frac{1}{(v_\mu l^\mu - ! - i'') (m^2 - l^2 - i'') [m^2 - (l - P)^2 - i'']} \\ &= \frac{1}{16\pi^2} \int_0^1 dx \left(\frac{s}{P^2} \frac{2}{2} + \tan^{-1} \frac{P^2}{s} + (s) \frac{1}{P^2} \log \frac{P^2 - s}{P^2 + s} \right) + \\ &+ \frac{1}{16\pi^2} \int_0^1 dx \frac{(s)^h}{P^2} \left(\frac{P^2}{s} + \frac{P^2}{s} \right) + \left(\frac{P^2}{s} \right)^i ; \end{aligned} \quad (23)$$

where $s = m^2 - !^2 + x(2!P_0 - P^2) + x^2(P^2 - P_0^2)$, $P_0 = v \cdot P$ and $! = ! - xP^2$. $I_0(!; v \cdot P; P^2)$ reduces to the integral $I_0(v \cdot P)$ given in appendix B of Ref. [20] in the limit $! = 0$ and $P^2 = 0$. This limit, however, is not applicable to the $pp \rightarrow pp^0$ reaction.

Our NNLO diagrams contain the usual divergences which need to be regularized and then renormalized by appropriate counter terms. The single-nucleon process (Born term) of Fig.1 (a) receives two types of corrections: (i) the "nucleon recoil corrections" of $O(m_N^{-2})$ involving nucleon known parameters, and (ii) the (infinite) loop corrections. The $\ell = 1$ loop corrections, $T_{\text{corr}}^{(+1)}$, to the Born amplitude were discussed in Ref. [13]. We denote by $T_{\text{corr}}^{(+2)}$ the $\ell = 2$ loop and recoil corrections to the Born term. The recoil corrections to the Born term are reduced by $(m_N - m_N)^{+2}$. The divergences contained in the graphs in Fig. 2 are canceled ("renormalized") by counter-terms in $L^{(2)}$ corresponding to the vertex (NNNN) vertex diagram (Fig.6). The same terms renormalize a part of the singularities in M_{IV} , Eq.(17), coming from Fig.3. The remaining singularities in M_{IV} are similar to those in the graphs in Fig.4. To eliminate the latter singularities, $L^{(2)}$ must contain further counter-terms of the π -nucleon scattering vertex type [21]. This can be accomplished with the use of these counter-terms in graphs similar to the one in Fig.5. We let $T_{\text{corr}}^{0(+2)}$ stand for the $\ell = 2$ transition operators that originate from such $\ell = 2$ counter-terms. The complete set of the $\ell = 2$ transition operators includes $T_{\text{corr}}^{(+1)}$, $T_{\text{corr}}^{(+2)}$, and $T_{\text{corr}}^{0(+2)}$, but we defer detailed discussion of these terms to a forthcoming paper [19] and concentrate here on the finite parts of the following effective operators²

$$T = T^{\text{Resc}} + T^{(+2)} : \quad (24)$$

d. Numerical results and discussion To proceed, we must fix the free parameters of the previous expressions. To NLO, as discussed in Ref. [13,14], the three parameters, c_1 , c_2 and c_3 of Eq.(6), enter into the pion rescattering operator T^{Resc} . We shall use the three sets of parameters employed in Ref. [15]. Sets A, B and C in Table 1 summarize these values. Set A

²Since we do not consider DW we leave out T^{Born}

represents the central values of c_1 , c_2 and c_3 determined in Ref. [20] using the experimental values of the pion-nucleon πN term, the nucleon axial polarizability χ_A and the isospin-even s-wave πN scattering length a^+ . Sets B and C represent typical ranges of allowed values in the current determinations of these parameters (see Ref. [13] for details).

For simplicity we limit our consideration to the threshold kinematics, which means $q = (m_\pi; 0)$ and the single exchanged boson (pion) of Fig. 1(b) has the four-momentum $k = (m_\pi; \vec{k})$ with $k^2 = m_\pi^2$. Then the initial nucleon three-momenta are $\vec{p}_i = 0$ (for nucleon $i = 1, 2$), and $(k; q)$ in Eq.(6) is fixed at [13,14]

$$q_{th} = \frac{m_\pi^2}{f^2} \left(2c_1 - \frac{1}{2}(c_2 + c_3 - \frac{g_A^2}{8m_N}) \right) : \quad (25)$$

Quantities of interest here are the magnitudes of the finite parts of the $\pi N \rightarrow \pi N$ transition operators, Eqs.(8)–(20), relative to the magnitude of the pion rescattering operator, T^{Resc} , Eq. (5). Let us denote these ratios³ by $R_K = M_K / T^{Resc}$ ($K = I, II, III, \dots, VII$). Table 2 gives R_K 's for each of the parameter sets A, B, and C. We note that R_I , R_{II} and R_{III} , corresponding to the graphs in Fig. 2, give quite substantial individual contributions but R_{II} and R_{III} cancel⁴ at threshold. Most remarkably, R_{IV} corresponding to the pion-pion rescattering diagram, Fig.3, is large, ranging 5–10.

The appearance of these large individual contributions calls for an explanation. The two-pion exchange diagrams in Fig. 2 can be viewed as a part of an effective π -meson exchange that Lee and Riska [4] found to be important in $pp \rightarrow pp\pi^0$. It has been shown via soft-pion arguments, e.g. in Ref. [23], that the effective π -meson exchange can be understood as a two-pion exchange. Although the few diagrams considered here are insufficient to generate the full strength of the isoscalar two-pion exchange between two nucleons, our NNLO results are indicative of the importance of the two-pion exchange diagrams for $pp \rightarrow pp\pi^0$. The diagram in Fig. 3 can be interpreted in two ways, either as a pion-exchange diagram [Fig. 1(b)] with a form factor attached to the N rescattering vertex, or as an effective π -exchange diagram wherein the exchanged π decays into two pions, one absorbed by the second nucleon and the other emitted as the outgoing π^0 . The large size of R_{IV} is consistent with this π -exchange picture.

The diagrams shown in Fig. 4 generate an effective form factors at the pion-nucleon rescattering vertex in $T^{(+1)}$. According to Table 2, the contributions of the corresponding operators, R_V and R_{VII} , are less than 20% and 15%, respectively. Thus, the higher chiral-order vertex corrections to $T^{(+1)}$ are found to be small, as expected from the general tenets of ChPT. Table 2 also indicates that R_{VII} is a small fraction, $R_{VII} = 0.1 - 0.2$, for all the cases studied. Again, this is consistent with the expectation that a $\pi = 2$ "recoil" correction to the $\pi = 1$ term ($T^{(+1)}$) should be small.

³ This type of comparison is possible because, at threshold, effectively only one kind of spin operator appears in the $pp \rightarrow pp\pi^0$ transition operator.

⁴ With DW this cancellation will not occur due to the different energy and three-momentum dependences.

Gedalin et al. [22] have considered some NNLO diagrams. Numerically, they found that the sum of (in our notation) M_{IV} and M_V is large. This feature is confirmed by our numerical result. It is worth emphasizing, however, that between these two transition operators M_{IV} is by far the predominant one. Although Gedalin et al. also considered M_{II} (our notation), they left out M_I and M_{III} . According to Table 2, M_{II} and M_{III} are of equal importance, and their individual contributions are comparable to that of M_{IV} . An additional remark is that our results contain a new loop-integral $I_0(!; v_p; p^2)$, Eq. (23), which does not appear in Ref. [22].

e. Conclusions We have evaluated the $pp \rightarrow pp^0$ transition operators to NNLO in chiral expansion. It was found that ChPT vertex corrections to the lower chiral order transition operators, T^{Born} and T^{Resc} are indeed small, as are the "recoil" corrections $O(m_N^{-2})$ to T^{Born} . Thus, for this limited type of diagrams, ChPT expansion seems to be under control. Meanwhile, the two-pion exchange contributions are found to be very large. This result is consistent with the expectation that the $pp \rightarrow pp^0$ reaction is sensitive to "heavy"-meson exchanges between nucleons. The phenomenologically important meson contributions [4] seem to have discernible "representatives" among the NNLO chiral perturbation diagrams considered here. It is not obvious whether one can interpret the large contributions from the individual graphs in Figs. 2 and 3 as evidence for the non-convergence of the ChPT expansion. These graphs appear for the first time in the NNLO calculations, and therefore the convergence question can only be settled by calculating corrections to these NNLO diagrams. We expect that the loop corrections to the individual diagrams in Fig. 2 will be smaller in magnitude. However, two-pion exchange diagrams of chiral order $= 3$ might have magnitudes comparable to our $= 2$ terms since the diagrams in Fig. 2 are only part of the effective π -exchange. To simulate a more realistic π -exchange it may also be necessary to include intermediate π in Figs. 2 and 3.

In a forthcoming paper [19] we shall present a detailed discussion of DW calculations necessary to obtain realistic cross sections for $pp \rightarrow pp^0$, as well as the details of the renormalization procedure at this level of approximation. Finally, we shall have to examine the corrections due to the use of the static heavy-nucleon "propagator" $1=(v \cdot p)$. These corrections can be estimated by replacing $1=(v \cdot p)$ with $1=(v \cdot p^2/(2m_N))$.

This work is supported in part by the National Science Foundation, Grant No. PHY S-9602000 and by the Grant-in-Aid of Scientific Research, the Ministry of Education, Science and Culture, Japan, Contract No. 07640405.

REFERENCES

- [1] H . O . M eyer et al., Phys. Rev. Lett. 65, 2846 (1990); Nucl. Phys. A 539, 633 (1992).
- [2] A . Bondar et al., Phys. Lett. B 356, 8 (1995).
- [3] G . A . M iller and P . U . Sauer, Phys. Rev. C 44, R1725 (1991); J A . N iskanen, Phys. Lett. B 289, 227 (1992)
- [4] T .-S . H . Lee and D . O . R iska, Phys. Rev. Lett. 70, 2237 (1993).
- [5] C . J . H orow itz, H . O . M eyer and D . K . G riegel, Phys. Rev. C 49, 1337 (1994).
- [6] E . Hernandez and E . O set, Phys. Lett. B 350, 158 (1995).
- [7] C . Hanhart, J . H aidenbauer, A . R euber, C . Schutz and J . Speth, Phys. Lett. B 358, 21 (1995); Acta Phys. Pol. B 27, 2893 (1996).
- [8] C . Hanhart, J . H aidenbauer, M . H o m ann, U .-G . M eissner and J . Speth, Phys. Lett. B 424, 8 (1998); C . Hanhart, J . H aidenbauer, O . K rehland J . Speth, Phys. Lett. B 444, 25 (1998).
- [9] R . Shyam and U . M osel, Phys. Lett. B 426, 1 (1998).
- [10] F . K leefeld and M . D illig, Acta Phys. Pol. B 29, 3059 (1998).
- [11] V . Bernard, N . K aiser and U .-G . M eissner, preprint nucl-th/9806013 (1998).
- [12] J . Adam , A . Stadler, M . T . Pena and F . G ross, Phys. Lett. B 407, 97 (1997).
- [13] B .-Y . Park, F . M yhrer, T . M eissner, J R . M orones, K . Kubodera, Phys. Rev. C 53, 1519 (1996).
- [14] T D . Cohen, J L . Friar, G A . M iller and U . van K olk, Phys. Rev. C 53, 2661 (1996).
- [15] T . Sato, T .-S . Lee, F . M yhrer and K . Kubodera, Phys. Rev. C 56, 1246 (1997).
- [16] U . van K olk, G . A . M iller and D . O . R iska, Phys. Lett. B 388, 679 (1996).
- [17] E . Jenkins and A . V . M anohar, Phys. Lett. B 255, 558 (1991).
- [18] S . W einberg, Phys. Lett. B 251, 288 (1990); Nucl. Phys. B 363, 3 (1991); Phys. Lett. B 295, 114 (1992).
- [19] V . D m itrasinovic K . Kubodera, F . M yhrer and T . Sato, in preparation.
- [20] V . Bernard, N . K aiser and U lf-G . M eissner, Int. J. Mod. Phys. E 4, 193 (1995)
- [21] N . Fettes, U .-G . M eissner and S . Steininger, Nucl. Phys. A 640, 199 (1998).
- [22] E . Gedalin, A . M oalem and L . Razdolskaya, preprint nucl-th/9803029 (1998).
- [23] G E . Brown and J . Durso, Phys. Lett. B 35, 120 (1971); G E . Brown, in "Mesons in Nuclei", eds. M Rho and D . W ilkinson (North-Holland, Amsterdam, 1979), 329.

TABLES

TABLE I. The three sets of $c_{1,2,3}$ parameters, in units of GeV^{-1} , used in the text.

| | c_1 | c_2 | c_3 |
|---|-------|-------|-------|
| A | 0.87 | 3.34 | 5.25 |
| B | 0.87 | 4.5 | 5.25 |
| C | 0.98 | 3.34 | 5.25 |

TABLE II. Sizes of the K^{th} type of diagrams, shown in Figs. 2 – 5, relative to the $\pi = 1$ pion rescattering diagram, Fig. 1 (b). The ratio R_K defined in the text is given for three sets (A, B and C) of parameters ($c_{1,2,3}$), see the text and Table I.

| | R_K^A | R_K^B | R_K^C |
|------------------|---------|---------|---------|
| $K = \text{I}$ | 0.70 | 0.38 | 0.53 |
| $K = \text{II}$ | 6.7 | 3.6 | 5.1 |
| $K = \text{III}$ | 6.7 | 3.6 | 5.1 |
| $K = \text{IV}$ | 9.5 | 5.1 | 7.2 |
| $K = \text{V}$ | 0.18 | 0.10 | 0.14 |
| $K = \text{VI}$ | 0.14 | 0.08 | 0.11 |
| $K = \text{VII}$ | 0.19 | 0.13 | 0.14 |

FIGURES

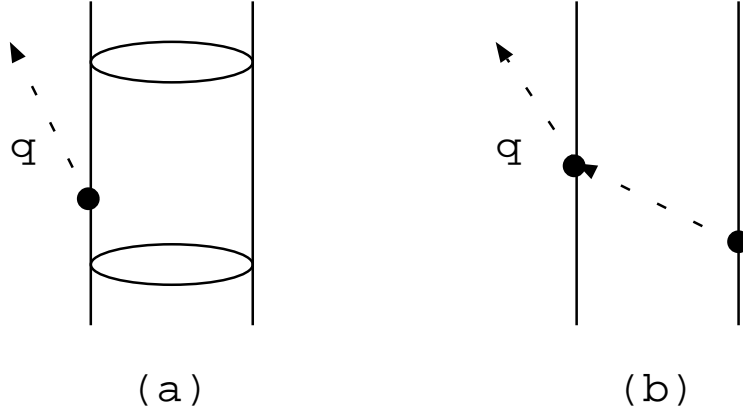
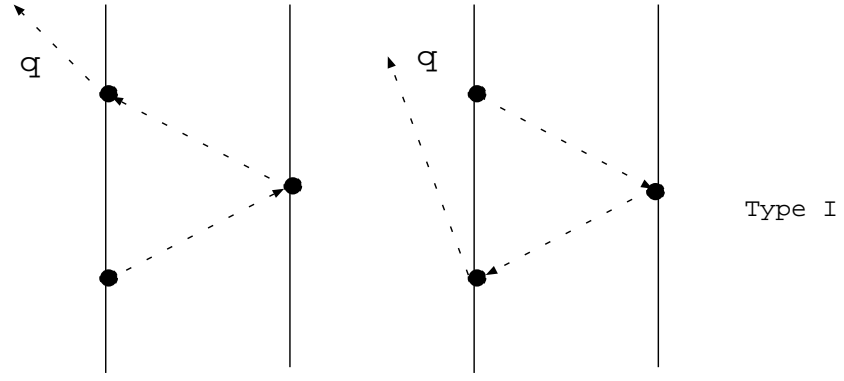
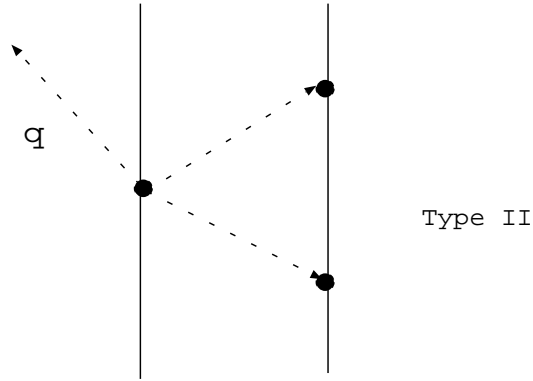


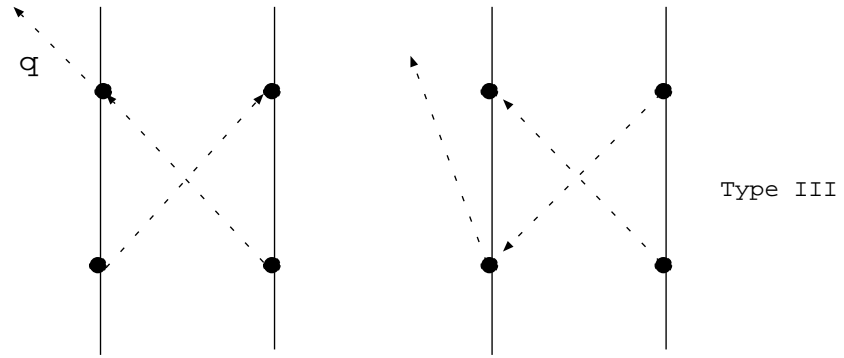
FIG. 1. Diagrams contributing to $pp \rightarrow pp^0$: Born term (a), the pion-rescattering term (b). The solid line denotes a nucleon (proton), the dashed line a pion and the open ellipses denote initial/final-state interactions.



(a)



(b)



(c)

FIG. 2. Two-pion exchange graphs of type I, II and III -the "cross-box" graphs.

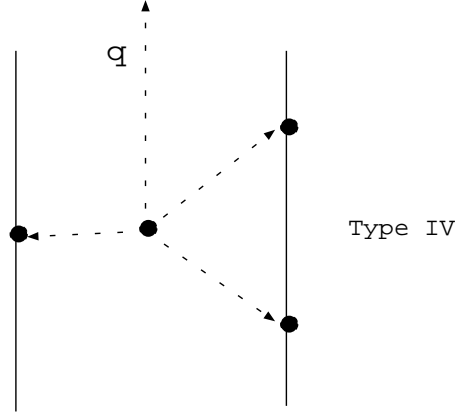


FIG .3. P ion-pion s-wave rescattering graph of type IV .

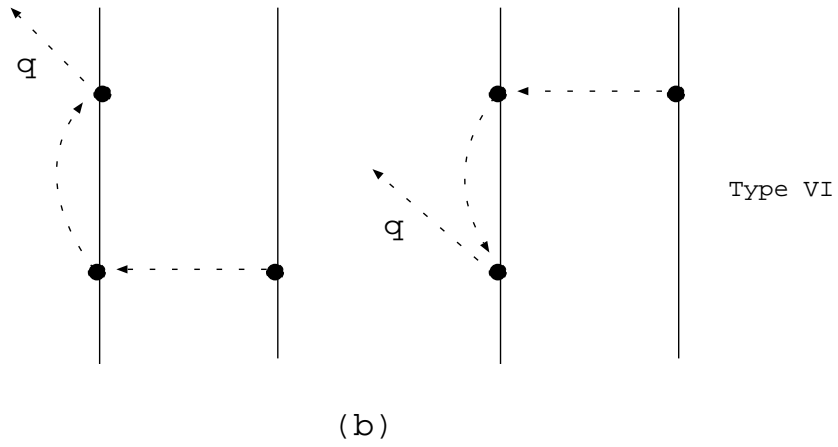
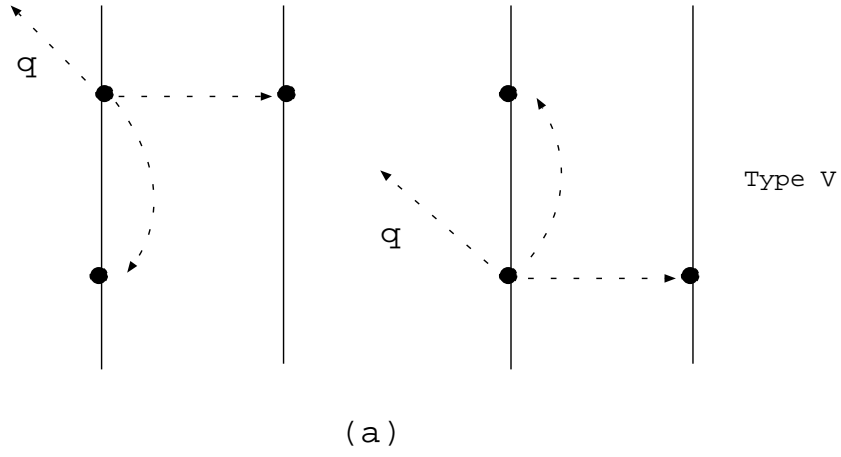


FIG .4. P ion rescattering vertex corrections to Fig.1 (b) of type V and VI.

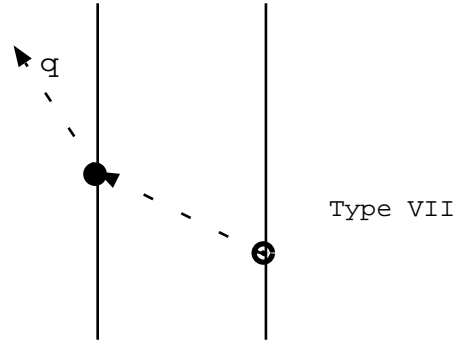


FIG . 5. The pion-rescattering graph with $\ell = 2$ at rescattering vertex.

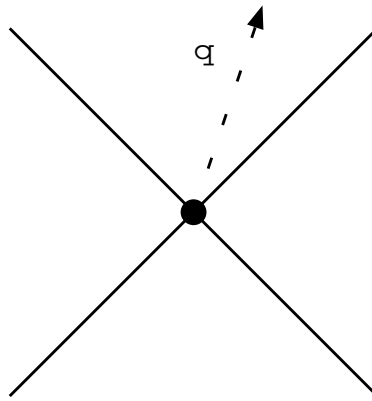


FIG . 6. The vertex contact-interaction counter-term graph.